MAGNETIC THRUST BEARING OPTIMIZATION STUDY

A Senior Thesis

By

Lawrence Lee

1996-97 University Undergraduate Research Fellow
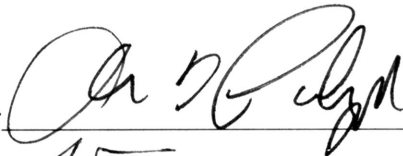
Texas A&M University

Group: ENGINEERING

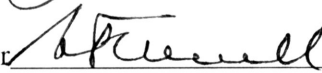Magnetic Thrust Bearing Optimization Study

Lawrence Lee
University Undergraduate Fellow, 1996-1997
Texas A&M University
Department of Mechanical Engineering

APPROVED

Fellow Advisor

Honors Director

Abstract

In industry today magnetic bearings are slowly replacing existing bearings because of its many advantages like less wear and environmentally clean. However, with all the advantages of MTB there are negative aspect in controlling the actuator and power losses associated with the bearing itself. These two drawbacks are the result of the eddy currents produced in these bearings, which are more pronounced in magnetic thrust bearings since the flux lines produced are perpendicular to the surface of the rotor . The report concludes that by slicing the stator into increasing the number of wedges that eddy currents are reduced and the phase lag decrease. The report will examine the difference between the static and rotating cases of magnetic bearings. The development of the dynamic magnetic bearing testing apparatus is fully detailed as well and at the time of this report was in the process of being manufactured.

Outline

Drawings - Bearing Housing I

Bearing Housing II

Stator Housing

Shaft

Base Plate

Modified Rotor

Nomenclature

β is a fringe factor varying between $0.9 - 0.95$

N is the number of turns in the wire

I is current passing through the wire

μ_o is the permeability of free space, $4\pi \times 10^{-7}$

μ_m^{rel} is the permeability relative to the material

l is the length of the current carrying wire

x is the position of the runner at static equilibrium position

g is the air gap when x = 0.

y deflection of the cantilever beam

P is force on the beam

x is length of the beam

a1 is location of applied force

E is modulus of elastitciy

I is area moment of inertia about neutral axis

δ is deflection

μ is coefficient of friction

a inner radius of the shaft

b outside radius of the shaft

c inner radius of bearing housing

Nomenclature (Continued)

l contact length between shaft and bearing

F_{mag} is magnetic force

P is pressure between the bearing and the shaft

$F_{friction}$ is friction force on the bearing

Introduction

Magnetic bearings are currently used in machinery ranging from turbomolecular vacuum pumps used in clean rooms to huge turbomachinery equipment used in power plants. Some advantages of magnetic bearings (MB) over conventional rolling element bearings include:

- less wear
- no lubrication system required
- environmentally clean
- adaptability to varying load and operating conditions
- improved performance at larger diameters- permitting use of less flexible shafs

With these advantages the number of applications where magnetic bearings are used is increasing.

In gas turbines, magnetic thrust bearings help reduce axial movement by keeping the turbine blades in place when gas forces push axially against the blades. The operating bandwidth frequency for these thrust bearings is normally low (<100 hz) because of eddy currents. In thrust bearings eddy currents produce a magnetic flux perpendicular to the surface of the bearing, which in turn induces phase lag, degrades the control of MTBs, and decreases stability. In addition eddy currents can overheat the shaft and produce braking torque because of the I^2R heating term.

The scope of this thesis is to concentrate on developing a more robust magnetic bearing control system and on eliminating eddy current effects in magnetic thrust bearing (MTB).

With the increasing number of magnetic bearings in use, there is an increasing need to have more precise and more accurate controls for magnetic bearing systems. If a

control system that offers total control is not developed then there exists a potential safety hazard when using a MTB system.

Literature Review

Eddy current effects of rotor-magnetic bearing systems and the importance of not neglecting eddy current effects have been discussed before in Kim, Palazzolo [reference]. In this paper new approaches and modeling of the magnetic bearings are taken into account. In addition, it is shown that surface conductivity affects the overall system stability. From this article, hiperco 27 is chose as the material used for the rotor and stator to help improve system stability.

Eddy currents produce a phase lag which prohibits suitable controls from being established for MTB in a dynamic environment. The phase lag that occurs in magnetic thrust bearings is documented in the paper by Baun, Fittro, Maslen, [1996]. Their paper examines and looks at force and current and air gap calibrations on a double acting magnetic thrust bearing. These calibrations are essential in terms of this thesis, since some of the calibration techniques are used for this static testing rig. In addition, high speed operations of eddy current dampers were discussed in a paper by Kilgerman, Grushkevich, and Darlow. They define the frequencies which it is optimal to use a eddy current damper.

This thesis builds on this research in an effort to minimize the eddy current and increase stability through different configuration types. The ultimate goal for this research would be the elimination the use of eddy current dampers all together at low or at high speeds.

Scope of Thesis

This thesis is divided into two sections the static testing rig and the dynamic testing rig. The static testing rig is described in full detail in terms of experimental apparatus, setup, as well as documentation on various errors made during testing procedure. The overall conclusions of the static testing rig are also noted. It was determined that the results were promising enough to warrant a look at a dynamic situation as opposed to a static one.

Still under development at the time of this report is the dynamic testing rig because it was still being built at the time of this report, little results are know. Preliminary calculations to design the apparatus are shown. In addition the experimental set up follows with the overall view of the apparatus after. However, the DTR is a more realistic operating environment for a magnetic thrust bearing. It is of extreme importance to see how the eddy currents effect the phase lag and hopefully compare these results to the STR in order to determine if a valid trend exists for wedge shaped stators.

Theory

The basic theory behind reducing eddy currents by increasing the number of wedges comes from work done by Schweitzon (1994) which is best illustrated in the following pictures.
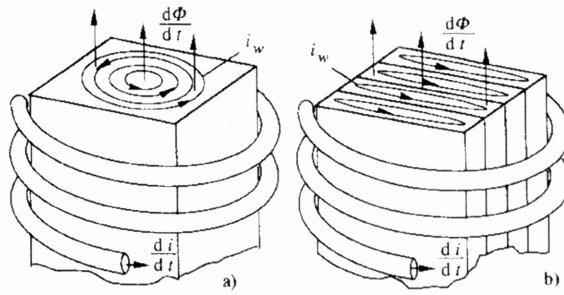
Figure 5 Eddy currents of a) magnetic core and b) divided magnetic core

Eddy currents are produced by the change in the magnetic flux denisity. When there exists a compact core the currents produce large eddy currents (Figure 5 a). Dividing the core as shown in Figure 5 b, prohibits large eddy currents from forming. Therefore, the more divisions in the core, the smaller the eddy current effects on the system.

The described theory above illustrates a sample of the work done by DeWeese in which this thesis is derived from. DeWeese's work on the static testing rig divides the stator into smaller and smaller wedge pieces of the static testing rig. In doing so hoping to reduce the phase lag of the overall system.

However, it is imperative to look at how the phase lag is created by these eddy currents.

The B field between the air gap is defined to be as follows:

$$B_{gap} = \left(\frac{NI/2}{(g+x)/\mu_o + l/\mu_o \mu_m^{rel}} \right) \beta \qquad \text{EQ 1}$$

Since the force of a magnetic field can be found using

$$F = \frac{B^2 A}{2\mu_o} \qquad \text{EQ 2}$$

and assuming that for a particular problem g = 0.025", l = 2", μ_m^{rel}=1,000 and combining

equations (1) and (2):

$$B(t) = \left(\beta \frac{N\mu_o}{2g} \right) I(t) \qquad \text{EQ 3}$$

Equation (3) provides a relationship for the magnetic field versus current, and it is this

equation that a lag time or phase lag is produced between the magnetic field and current

at high frequencies. Therefore, a complete frequency sweep is needed in order to

determine the phase lag produced by eddy currents.

Basically the dynamic testing apparatus theory constitutes the same theory as the

STR; however the rotor in rotating now.

Experimental Setup - Static Testing Rig

The following diagram, Figure 1, is the setup used for the static test rig. Most of

the equipment was already at Dr. Palazzolo's lab since Mr. DeWeese had done his thesis

there.
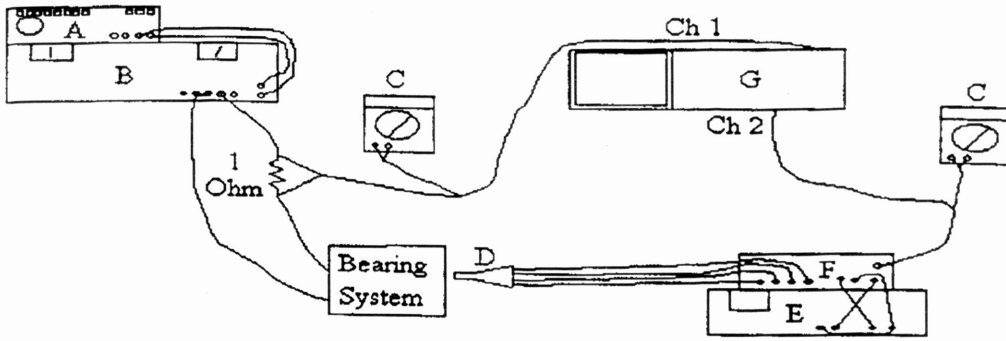
Equipment List
A - Wavetek Function Generator
B - Kepco Bipolar Operational Power Supply/Amplifier
C - Mulitmeter
D - Hall Probe
E - Tri Output Power Supply For Hall Probe
F - Hall Probe Controller
G - Spectral Dynamics Signal Analyzer

Figure 1. Experimental Setup STR (picture taken from DeWeese)

A closer look at the magnetic bearing system is needed in order to fully understand the
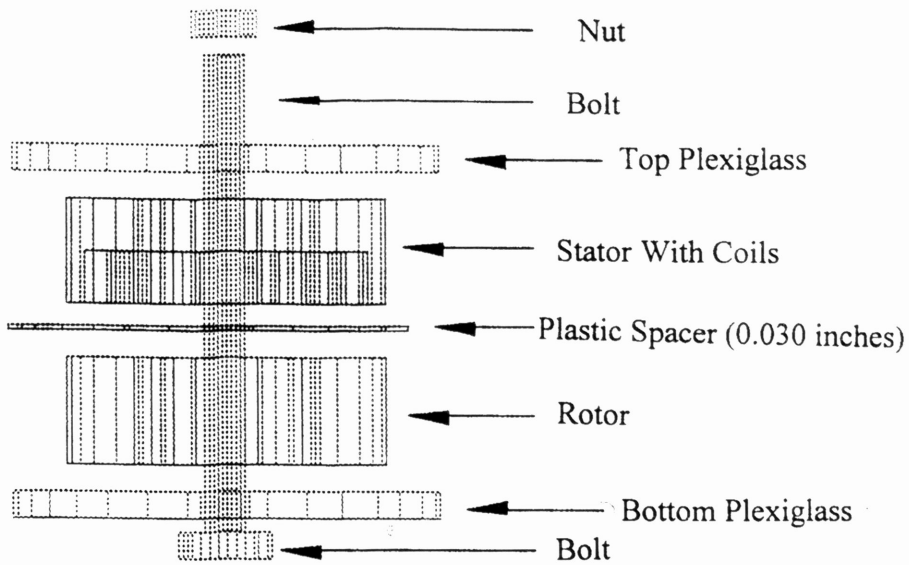
the complete experimental setup.

Figure 2. Exploded View (picture taken from DeWeese)

The plastic spacer in Figure 2 prevents other wedge pieces from interfering with the magnetic flux detected by the hall probe. Plastic shims are also placed between each wedge piece to prevent eddy currents from conducting into each wedge. Figure 3 shows this in more detail.
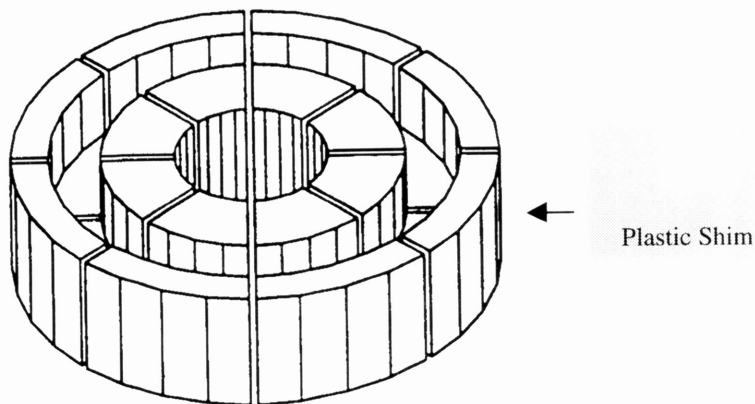

Figure 3 Stator after being cut into wedges with shim

Experimental Procedure

Before tests for the flux density and phase lag could be performed, the circuit and magnetic system were set up, the Kepco power supply was turned on, and the function generator was set to 10.0 ± 0.5 hertz. The DC and AC currents(RMS) were set while the frequency was set at 10.0 hertz. Using a multimeter to monitor the DC input voltage, the input voltage was set to 0.5 volts. The AC current (RMS) was switched on and set to approximately one half of the DC current. The AC current was always less than the DC current to ensure **a** positive bias remained in the circuit. Magnetic flux was measured using the multimeter and a hall probe. The hall probe was placed inside the gap and was moved until the multimeter read the highest reading. To ensure a sinusoidal form, the signal analyzer was set in the time domain for both wave forms and both forms were observed using the signal analyzer. The transfer function and the phase lag between the two signals are determined by switching the signal analyzer from time to frequency domain. After the magnetic flux signal is divided by the input signal analyzer plots the phase lag and the magnitude of the transfer function.

Results of static testing rig

After setting up the apparatus and the experiment, several tests were run and varying results were found between the different runs of the experiment. Table 1 lists the results of these tests which show no consistent trend. The phase lag represents how much the phase of the current and magnetic field differ. The transfer functions measures the amount of magnetic flux produced by the voltage applied to the experiment apparatus. The transfer function is analogous to an efficiency of the overall system.

Table 1. Sixteen wedged stator results for Co-Fe at 100.0 hertz

Trial number and date	Results (phase lag [Degrees], transfer function [KG/Amp])	Reason
1 - Oct 6th	-18°, 0.359	Not tightened, not isolated, PND
2 - Oct 6th	-3°, 0.0979	Not tightened, isolated, PND
3 - Oct 12th	-8°, 0.381	Not tightened, isolated, PND
4 - Oct 12th	-8°, 0.381	Not tightened, isolated, PND
5 - Oct 12th	-18.6°, 0.364	Tightened, isolated, PWD
6 - Oct 12th	-16.5°, 0.362	Tightened, isolated, PND
7 - Oct 12th	-16.9°, 0.376	Tightened, not isolated, PND

PND – Probe on narrow side of disk
PWD – Probe on wide side of disk

The variation in the results listed in Table 1 was because of several reasons. First, wires had not been correctly tightened, and the bolts of the magnetic bearing system did not compress the Plexiglas to prevent system vibration. Table 2 lists the results of the 16 wedge stator configuration and the other wedge stator configurations tried by Randy DeWeese.

Table 2. Solid and wedged stator results for Co-Fe at 100.0 Hertz

Stator Configuration	Transfer Function [KG/Amp]	Phase Angle [Degrees]
Solid*	0.430	-23.50
Wedge(8)*	0.372	-19.00
Wedge(16)	0.376	-16.9

* Based on Previous Work by Randy DeWeese

The results in table above prove that as the number of wedge pieces, increases the phase angle decreases. The reason why the transfer function increases instead of decreasing on the last entry reading is not known. Further research is needed to determine if a trend exists for the transfer function. Of the two, phase angle and transfer function, phase angle

is the more important component of the two. The stator was not further divided in 32 because the dynamic testing rig needed concentrated analysis.
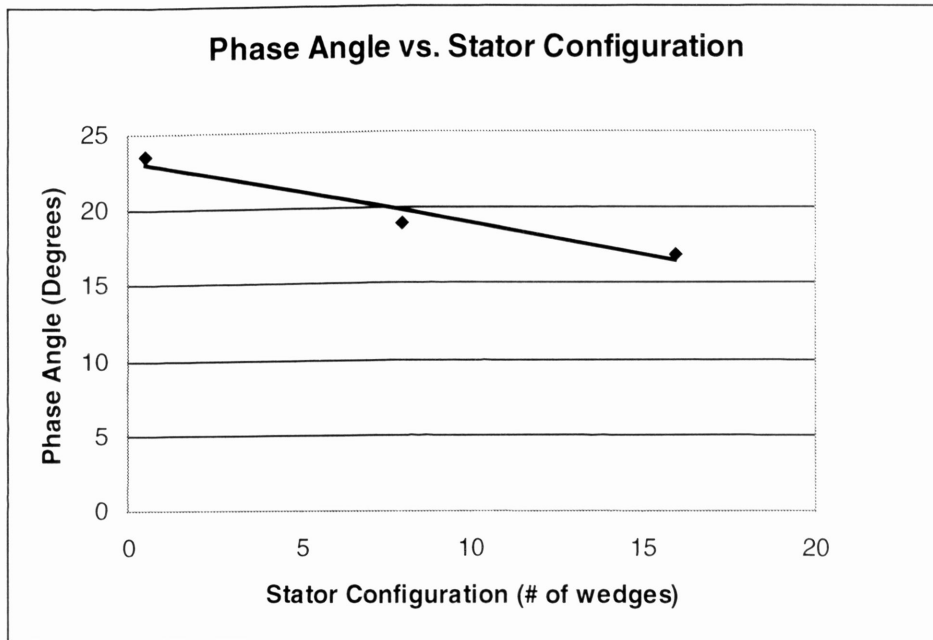
Phase Angle vs. Stator Configuration

Figure 4 shows the phase lag compared to the wedge stator configuration.

The general trend from Figure 4 shows exactly what was predicted by Schweitzon, the more wedge pieces, the smaller the eddy current effects, and consequently the smaller the phase angle lag between the rotor and the stator. The polynomial trend line is able to fit all three points exactly, however, this is in accurate

Preliminary Calculations

In developing a new experimental apparatus, many preliminary calculations had to be examined.

The first step is determining the force created by the magnetic circuit in the dynamic

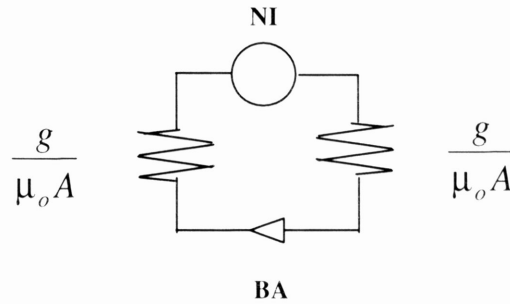testing apparatus. The apparatus becomes the following magnetic circuit:

Figure 6 - Analogous Magnetic Circuit used to examine Magnetic Force of DTA

From the above circuit the following equation is derived

$$BA\frac{2g}{\mu_o A} = NI \qquad\qquad \text{EQ 4}$$

Magnetic flux reduces to the following:

$$B = \frac{\mu_o NI}{2g} \qquad\qquad \text{EQ 5}$$

The overall Force of a magnetic field is calculated by:

$$F = \frac{B^2 A}{2\mu_o} \qquad\qquad \text{EQ 6}$$

However, the magnetic force is multiplied by two since the field works on both the rotor

and the stator. Substituting EQ 5 into EQ 6 results in the following force on the

experimental system:

$$F = \frac{\mu_o N^2 I^2}{4g^2} \qquad\qquad \text{EQ 7}$$

Calculated force using these formulas are approximately 260 lbs. In order to increase the factor of safety 400 lbs. was used as maximum force created by the magnetic bearing on the shaft.

Other design calculations needed to ensure proper test results safety and overall reliability.

Given that the force is 400 lbs. the deflection on each of the housings needed to be calculated. Each was assumed to be analogous to a cantilever beam. Since the force placed on this "beam" is located with in the given length then

$$y = \frac{P}{6EI}\left(3a^2 x - a^3\right) \qquad\qquad \text{EQ 8}$$

The deflection using the assumption that the housings were cantilever beams was very minimal and in the order 10^{-5} in. The calculation was done for both stator and bearing housings.

Upon satisfaction with the size of deflection, attention was turned to the amount of interference need in order to maintain the shaft from slipping out of the bearing housing. The pressure needed to keep the bearing and shaft together are as follows (Shigley 1977)

$$P = \frac{E\delta}{b}\left[\frac{\left(c^2 - b^2\right)\left(b^2 - a^2\right)}{2b^2\left(c^2 - a^2\right)}\right] \qquad\qquad \text{EQ 9}$$

Knowing that the pressure can be redefined as the following:

$$P = \frac{F_{friction}}{\mu(2\pi cl)} \qquad\qquad \text{EQ 10}$$

In order to incorporate another factor of safety, an assumption was made for $F_{friction}$ to be three times F_{mag}. From Serway μ is approximately 0.57 for metal on metals, and "a" term becomes zero since the shaft is solid and not hollowed out. With these modifications than EQ R and EQ S can be combined to fine the necessary δ with the following equation:

$$\delta = \frac{3F_{mag}b}{2\pi\mu lE}\left[\frac{2(c)}{\left(c^2 - b^2\right)}\right] \qquad\qquad \text{EQ 11}$$

A retaining plate holds the bearing into the housing. This plate had several screw and in order to determine if the screws could withstand the axial force placed on the bearing the following calculation needed to be done:

$$\sigma_{screw} = \frac{F_{mag}}{\#\_of\_Screws * A_{surfaceofscrew}} \qquad\qquad \text{EQ 12}$$

If the σ_{screw} is less than the prescribed stress on a individual bolt, then the bolts should withstand the force. After doing the calculations, it was shown that all bolts could withstand the prescribed force.

Experimental Setup for Dynamic Testing Rig

After making several calculation and various drawings to redefine the experiment the following assembly drawing (Figure 7) was created.
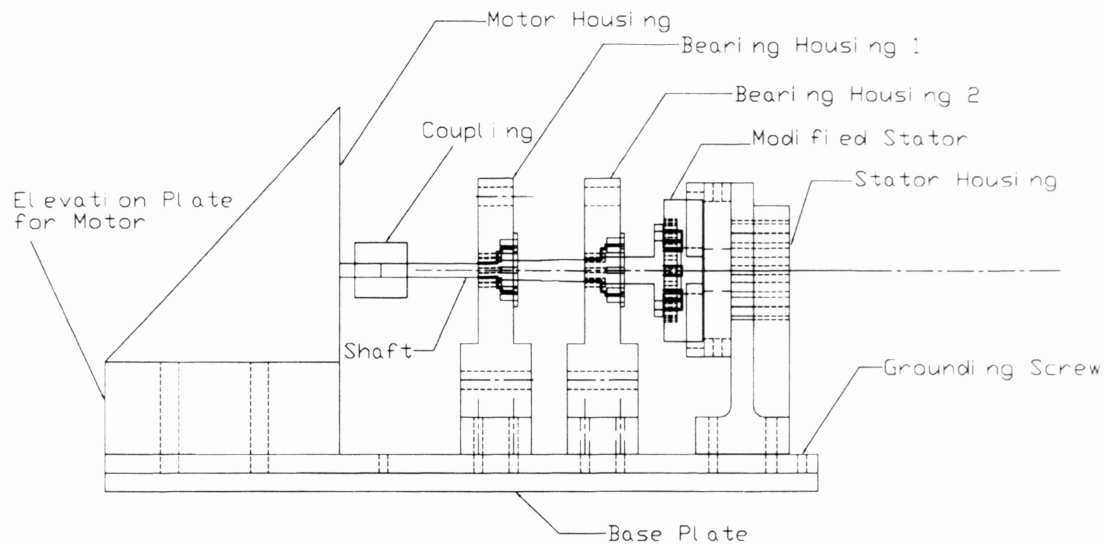
Figure 7 . Assembly drawing of Dynamic Bearing System

At the time of this report the DTR was still being completed. There results of this

appended onto the report once the result are found.

The motor will be turning at a rate of 10,000 rpm. A speed controller is need as

well to make sure the motor will turn at the desired speed. The Hall Probe will still be

used to monitor the magnetic flux from the eddy currents. The Wavetek Function

Generator, Kepco Bipolar Operational Power Supply, Mulitimeter, Tri Output Power

Supply, Hall Probe Controller, and Spectral Dynamics Signal Analyzer will be used in the

same fashion as the STR.

Expected Results

The main goal of the DTR is to take the results from the STR to the next logic

step. Examining the stator wedge configuration in a dynamic environment seeing how

the eddy currents effect the system in terms of phase lag. The DTR is indeed more important due to the fact more thrust bearings act in this fashion
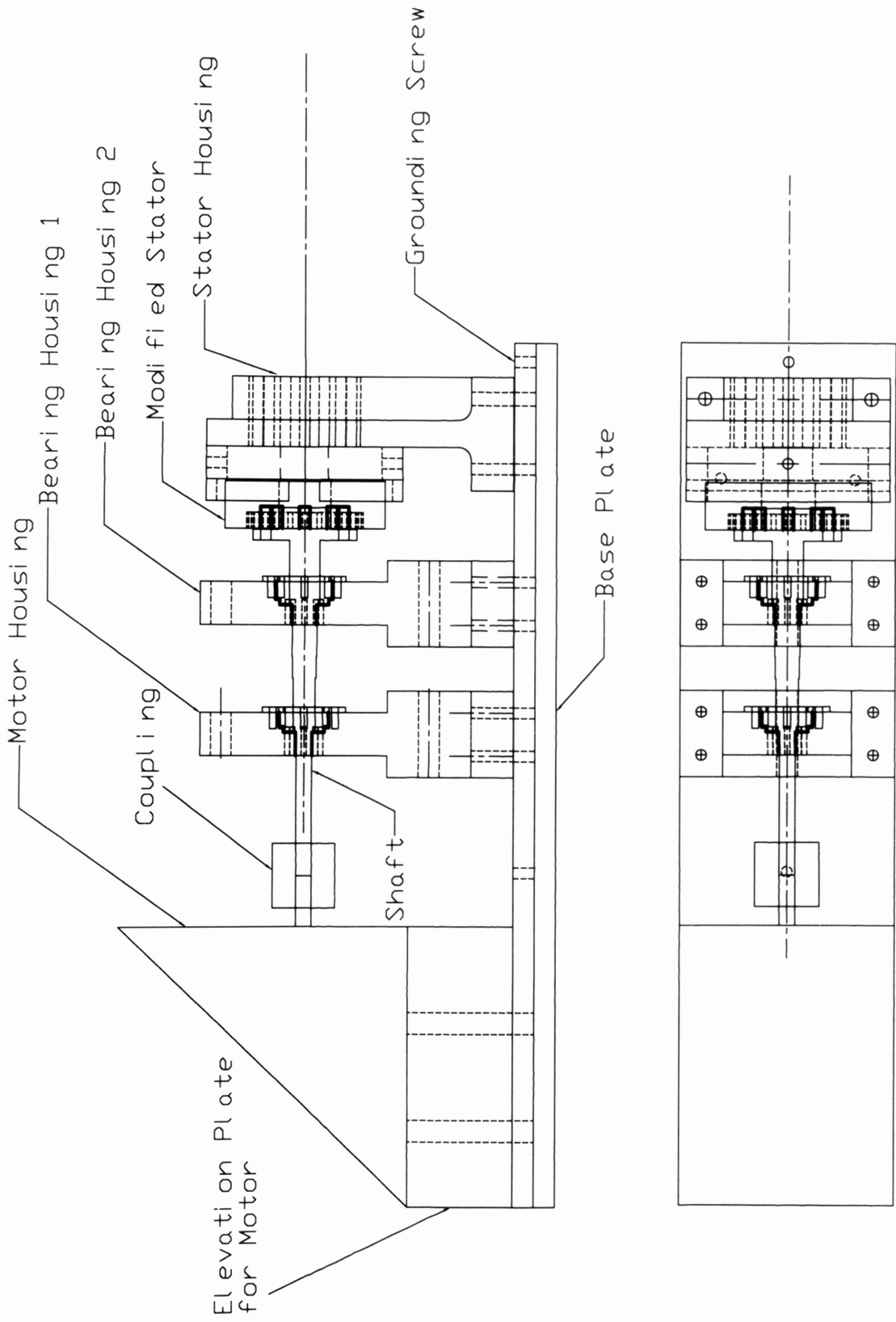
Future Work

Another stator made of Hiperco 27 will be cut to be tested in a dynamic testing rig. In order to determine if an increase in wedge sections will increase or decrease the phase angle.

In addition based on work done by DeWeese, other stator configuration that performed well in the STR will be tested in the DTR.
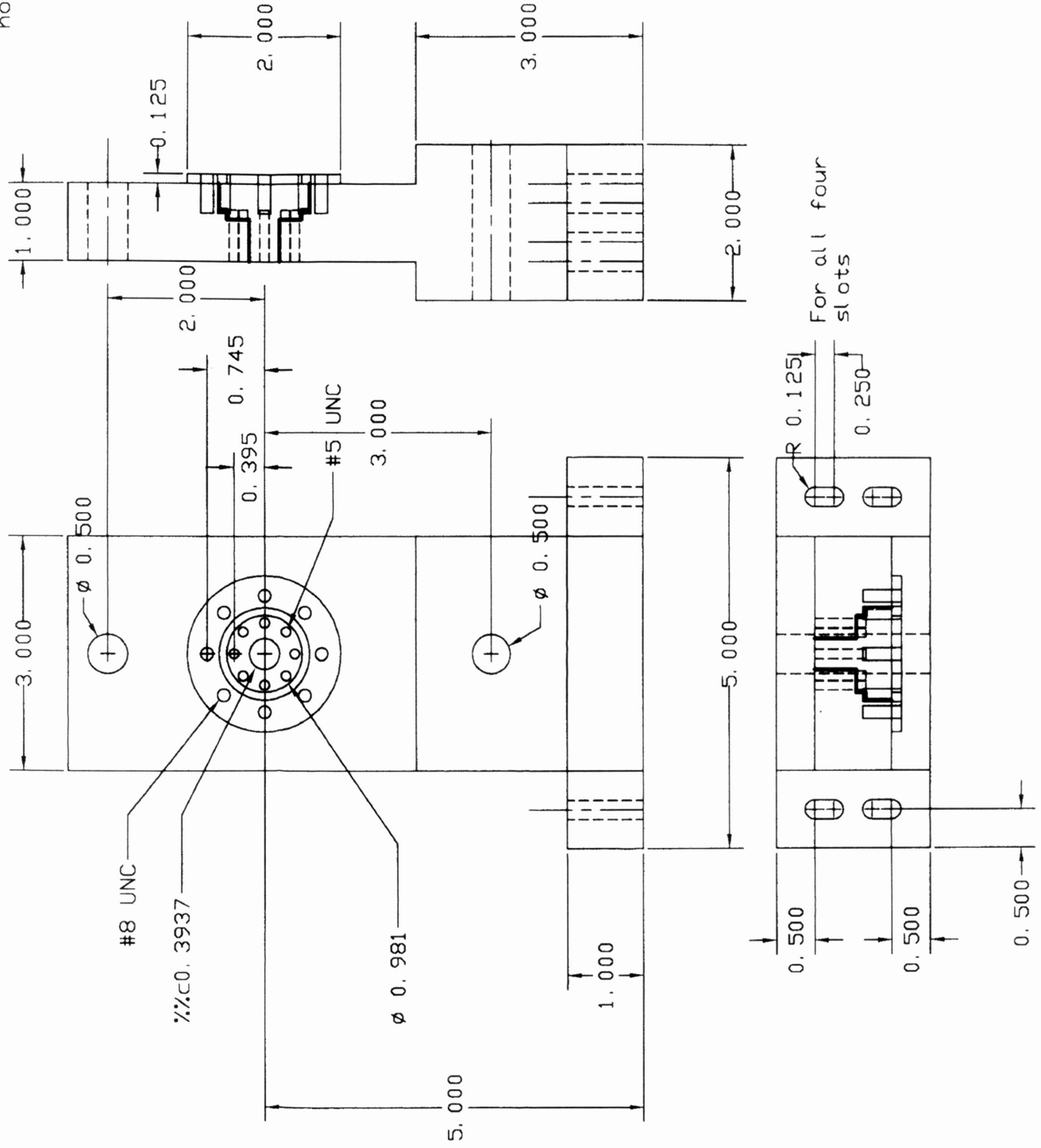
References

Baun, D.O., Fittro, R.L., Maslen, E.H. 1996, "Force Versus Current and Air Gap Calibration of a Double acting Magnetic Thrust Bearing," *Transactions of the ASME*, Birmingham, UK

DeWeese, R., "A Comparison of Eddy Current Effects in a Single Sided Magnetic Thrust Bearing, " *Masters Thesis*, Texas A&M University, Department of Mechanical Engineering.

Kilgerman, Y., Grushkevich, A., and Darlow, M. 1995, "Analytical and Experimental Evaluation of Instability in Rotordynamic System with Electromagnetic Eddy-Current Damper," *Journal of Vibration and Acoustics*.

Kim, C., Palazzolo, A.B. 1995, "Eddy Current Effects on the Design of Rotor-Magnetic Bearing Systems," *Transactions of the ASME*.

Schweitzer, G., Bleuler, H., Traxeler, A. 1994, "Basics, Properties and Applications of Active Magnetic Bearings, " *Active Magnetic Bearings*, Hochschulver, Zurich, Switzerland, pp. 1-112.

Shigley, Joseph Edward. 1977, Mechanical Engineering Design, McGraw-Hill, New York, New York, pp. 63-66.

Serway, Raymond A. 1990, Physics For Scientists and Engineers, Saunders Golden Publishing, Philadelphia, PA, pp 113.
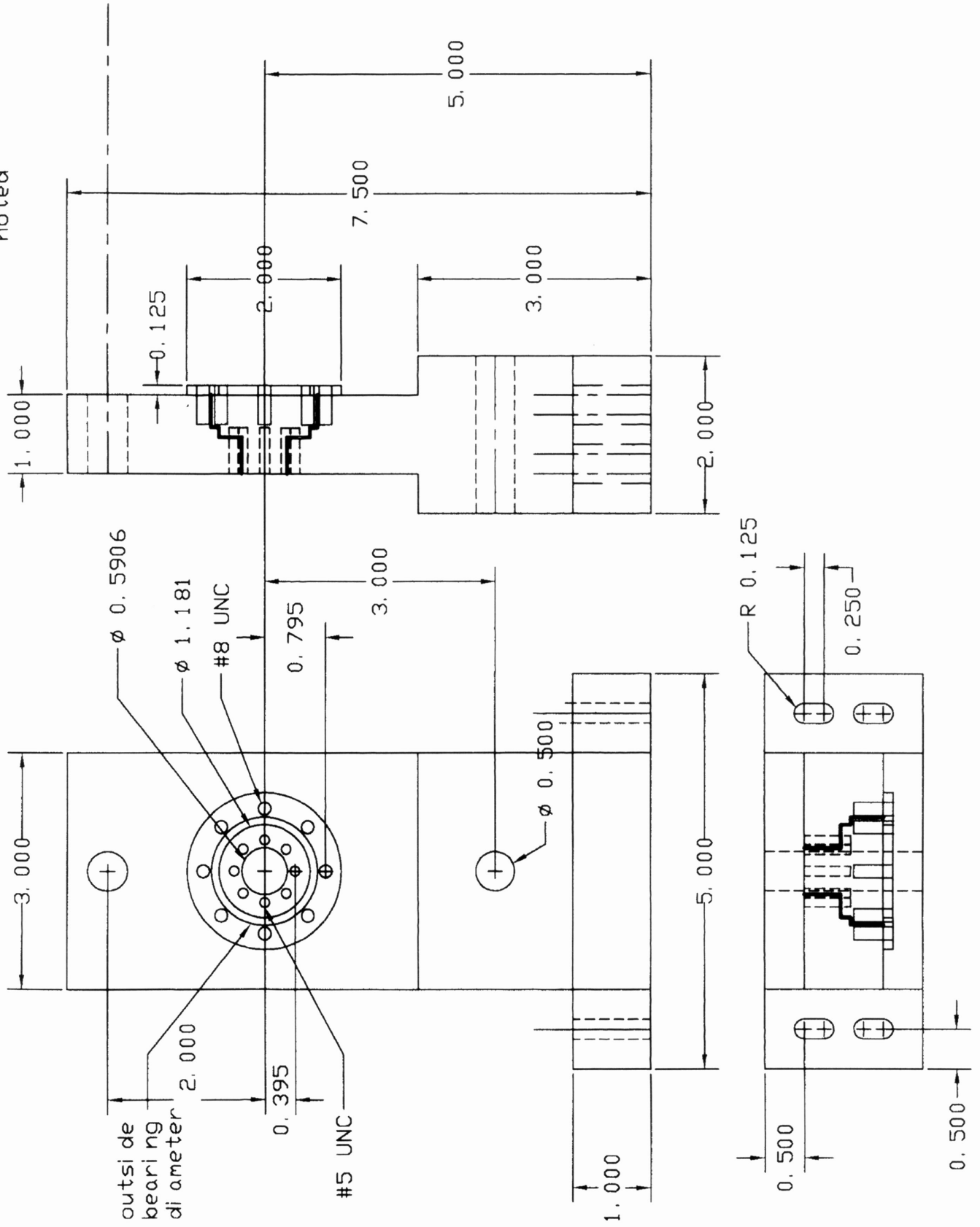
Appendix

Motor Housing

Bearing Housing 1

Bearing Housing 2

Modified Stator

Stator Housing

Grounding Screw

Coupling

Shaft

Base Plate

Elevation Plate
for Motor

Bearing Housing 1 — Mild Steel

Tolerance +/- 0.015 unless otherwise noted

2.000

3.000

0.125

1.000

2.000

2.000

0.745

0.395

#5 UNC

3.000

ø 0.500

ø 0.500

3.000

5.000

For all four slots

R 0.125

0.250

#8 UNC

%%c0.3937

ø 0.981

1.000

0.500

0.500

0.500

5.000

5.

Bearing Housing 2 - Mild Steel

Tolerance
+/- 0.015 unless
otherwise
noted

5.000

7.500

2.000

0.125

3.000

1.000

2.000

Ø 0.5906

Ø 1.181

#8 UNC

0.795

3.000

Ø 0.500

outside
bearing
diameter

2.000

0.395

#5 UNC

5.000

1.000

R 0.125

0.250

0.500

0.500

0.500

Rotor Housing - Plexiglass

0.500
2.000

5.000

Ø 0.250

1.875

1.250

0.500

2.625
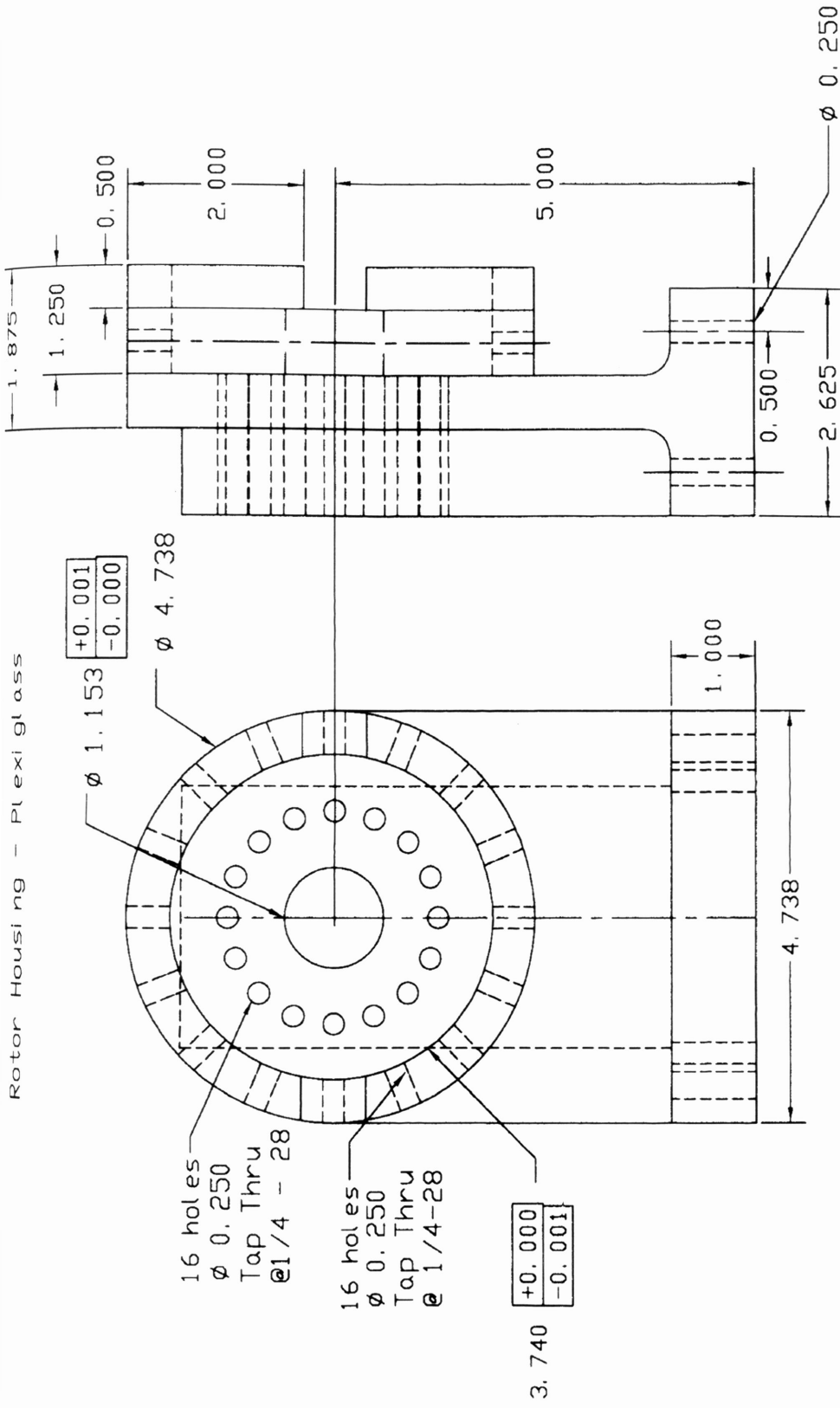
Tolerances
+/- 0.015
unless otherwise
noted

2.875

1.000

0.500

Ø 1.153 | +0.001 | -0.000 |

Ø 4.738

0.500

1.000

0.500

0.434

0806

1.000

4.738

16 holes
Ø 0.250
Tap Thru
@1/4 - 28

16 holes
Ø 0.250
Tap Thru
@ 1/4-28
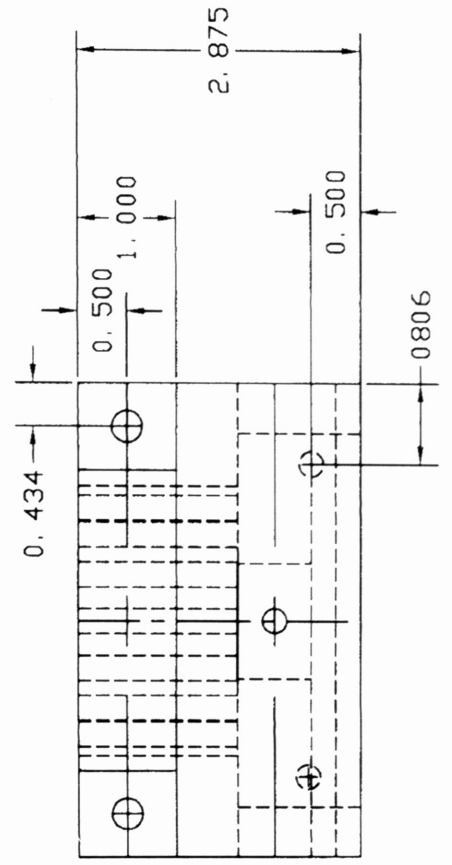
3.740 | +0.000 | -0.001 |

shaft

housing 1 range [.56-.50]
housing 2 range [.75-.69]

Ø 1.250

Ø0.2500

Ø 0.125
4 holes
tap thru

0.9375

0.315

8 holes
#14 fine

Ø 2.500

0.250

0.500

0.500

1.500
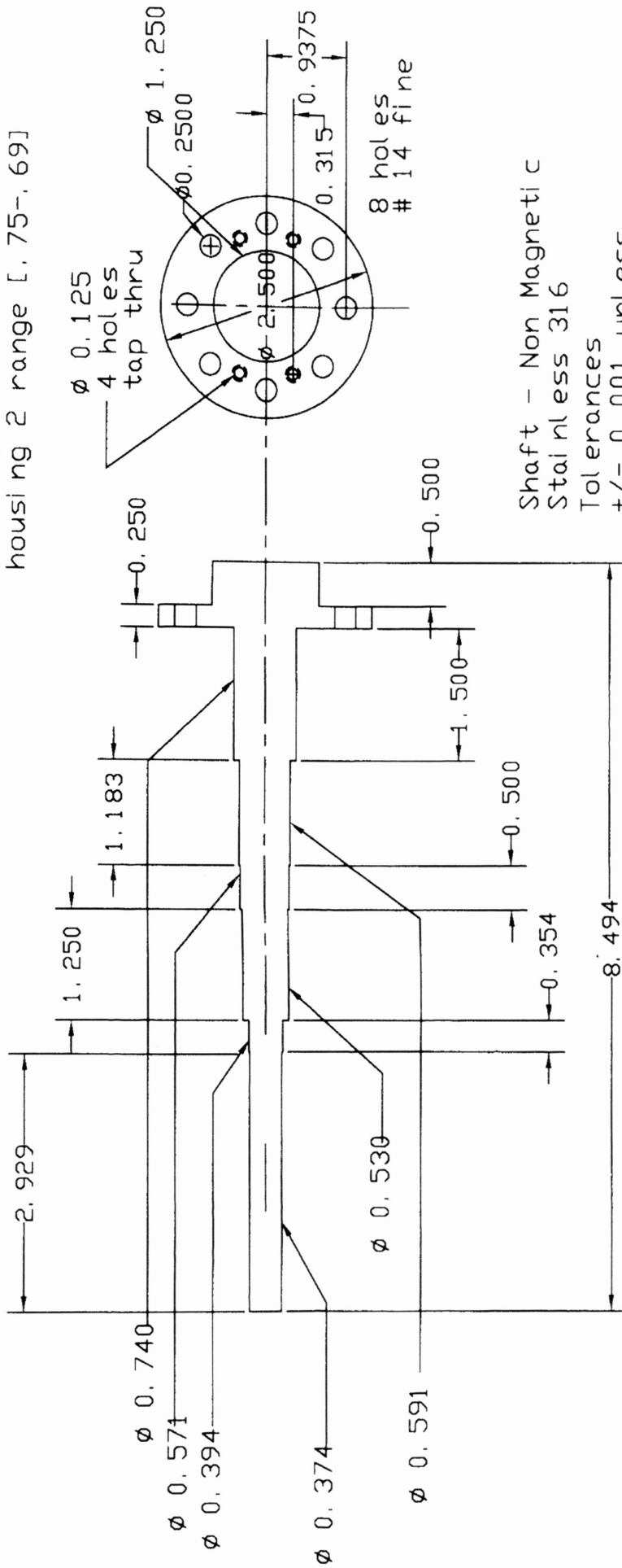
Shaft - Non Magnetic
Stainless 316
Tolerances
+/- 0.001 unless
otherwise
noted

1.183

1.250

0.354

2.929

8.494

Ø 0.530

200K 0.3937 +0.0003
202K 0.5906 +0.0003

bore

Ø 0.740

Ø 0.571

Ø 0.394

Ø 0.374

Ø 0.591
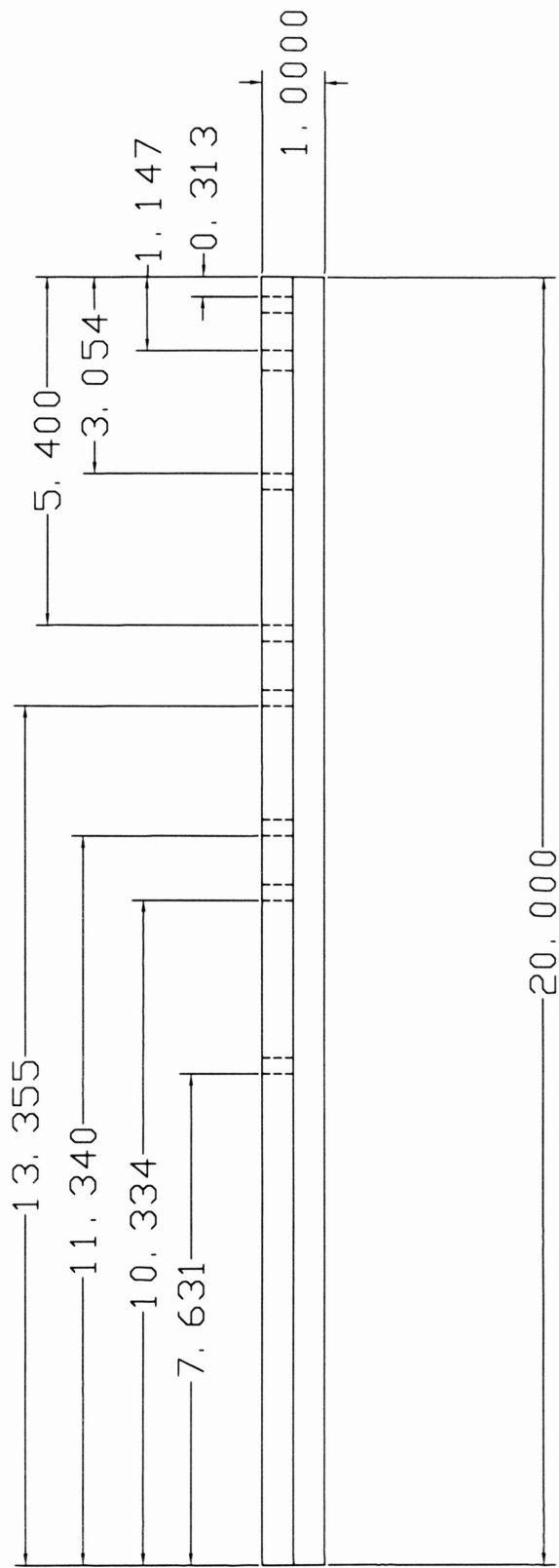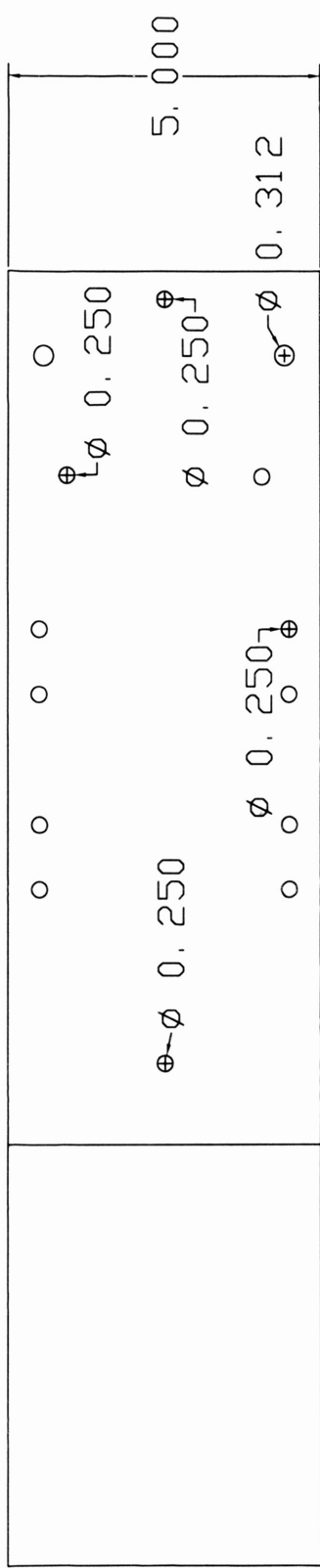
Tolerance
+/- 0.015 unless
otherwise specified

#14 UNF
8 holes

0.375

0.500

1.087

0.938

3.8570

1.342

Ø1.250

#4 UNF